ac Stark effect in a doubly driven three-level atom

Changjiang Wei,[1,2] Dieter Suter,[2] Andrew S. M. Windsor,[1] and Neil B. Manson[1]
[1]*Laser Physics Center, The Australian National University, Canberra, ACT 0200, Australia*
[2]*Fachbereich Physik, University of Dortmund, Dortmund 44221, Germany*
(Received 19 March 1998)

In this paper we present a detailed treatment of the ac Stark effect of a three-level atom driven by two strong laser fields in a cascade scheme. We consider two situations where there is a weak laser field probing a new transition starting from one of the three levels to a fourth level. In one case the initial level of the probed transition is the ground state and in the other case the initial level is the intermediate state. For both situations we derive an analytical expression for the absorptive and dispersive responses of the weak probe field and present the spectrum obtained from numerical calculation. The general feature of the spectrum has a three-peak structure. The positions and relative intensities of the three spectral components are affected strongly by the driving field intensities and detunings. An account of the spectrum is given in terms of the dressed-state formalism. [S1050-2947(98)04709-X]

PACS number(s): 32.80.−t, 42.50.Hz, 42.62.Fi, 42.65.−k

I. INTRODUCTION

The interaction between a two-level atom and a strong laser field is one of the most extensively studied subjects in quantum optics and laser spectroscopy [1–3]. It is the simplest model available for studying atom-photon interactions and yet accounts for many interesting observations, such as Mollow triplet, ac Stark splitting, and gain without population inversion [4–14]. With the growth of experimental sophistication, many new and more complex nonlinear behaviors associated with multilevel atoms interacting with multifrequency laser fields have been considered and such a case is the subject of the present paper. The most thoroughly studied situation is that of a three-level atom interacting with two laser fields. In comparison to the two-level atom, the three-level atom represents more possible configurations for laser interaction including V, Λ, and cascade schemes. In addition, in many cases of interest its theoretical analysis can be simpler than that for the two-level atom [15]. Using a pump-probe spectroscopy method, where the pump field has a fixed frequency and its effect is examined by recording the response of the three-level atom as a function of probe field frequency, many interesting effects have been observed, such as ac Stark splitting (also known as Autler-Townes splitting [16]), coherent population trapping, electromagnetically induced transparency, amplification, and lasing without population inversion [17–36]. More recently, by driving one of the transitions with two strong pump fields, multipeak ac Stark splitting has been observed [37–40]. A comprehensive review of the ac Stark splitting of a three-level atom in the presence of two strong pump fields can be found in recent papers by Narducci and his collaborators [41,42].

In all of the investigations mentioned above the effects have been measured by monitoring transitions within the driven three-level atom. In this paper we consider the ac Stark splitting of a three-level atom subjected to two pump fields in a different situation where there is a weak field probing a new transition starting from one of the three levels to a fourth level. This is a configuration consisting of a four-level atom interacting with two pumps and one probe (see Fig. 1). The motivation for the present work originates from the classical papers by Cohen-Tannoudji and Reynaud, which are concerned with fluorescence and absorption spectrum of a strongly driven atom under various configurations [43–45]. In particular, they studied a three-level atom interacting with two strong pump fields in a cascade scheme and predicted a three-peaked absorption spectrum [45]. Because the purpose of these papers was to present the dressed-state concept for describing atoms in a strong laser field, the discussion was focused on predicting the general pattern of the fluorescence and absorption spectrum. The actual spectrum, however, was not calculated and the discussion was restricted to the case where both pump fields were resonant [45]. There are also other recent relevant studies which are

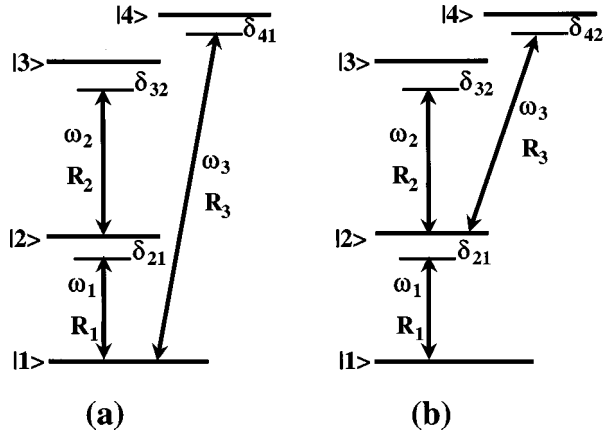

FIG. 1. A three-level atom driven by two strong pump fields in a cascade scheme whose ac Stark effect is studied by probing a new transition starting from either (a) the ground-state level $|1\rangle$ or (b) the intermediate level $|2\rangle$ to a fourth level $|4\rangle$. ω_1 and ω_2 are the pump field frequencies, R_1 and R_2 are their corresponding Rabi frequencies. ω_3 is the probe field frequency and R_3 is its Rabi frequency. The pump field detunings are given by $\delta_{21}=\omega_1-\omega_{21}$ and $\delta_{32}=\omega_2-\omega_{32}$. The probe field detuning is (a) $\delta_{41}=\omega_3-\omega_{41}$ and (b) $\delta_{42}=\omega_3-\omega_{42}$.

directed to some particular processes including absorption within an electromagnetically induced transparency window [46] and laser-induced transparency and dark-line effects caused by three-wave mixing in atomic systems [47]. The purpose of this paper is to present a numerical calculation of the absorption and dispersion profiles of a weak field which probes the doubly driven three-level atom to a fourth level (see Fig. 1). In the limit of weak probe, an analytical expression is derived perturbatively for cases where the initial level of the probed transition is either the ground-state level or the intermediate level of the three-level atom. The absorption and dispersion profiles are calculated for various parameters including the intensities and detunings of the driving fields. We show that the general feature of the ac Stark effect of the doubly driven three-level atom is a spectrum with a triplet structure. We also discuss the general pattern of the absorption and dispersion profiles in terms of the dressed-state formalism.

This paper is organized as follows. In Sec. II we derive analytical solutions for the absorption and dispersion profiles by solving the density matrix equation of motion to first order of the weak probe field. In Sec. III we introduce the dressed-state formalism for a three-level atom driven by two strong fields. Using the solutions given in Sec. II the absorption and dispersion profiles are calculated numerically and the results are presented and discussed in Sec. IV. Also included in Sec. IV is the discussion of the general pattern of the absorption and dispersion profiles using the dressed-state formalism in comparison to the numerical results. Finally, the paper is summarized in Sec. V.

II. FIRST-ORDER SOLUTION OF THE DENSITY MATRIX EQUATION OF MOTION

We consider a three-level atom with a ground state $|1\rangle$ and excited states $|2\rangle$ and $|3\rangle$ in the presence of two strong pump fields with frequencies of ω_1 and ω_2 in a cascade configuration as depicted in Fig. 1. The $|1\rangle\rightarrow|2\rangle$ transition of frequency ω_{21} is driven by the pump field ω_1 with a Rabi frequency of R_1. The $|2\rangle\rightarrow|3\rangle$ transition of frequency ω_{32} is driven by the pump field ω_2 with a Rabi frequency of R_2. Assuming that such a doubly driven three-level atom is probed to another excited state $|4\rangle$ with a weak field ω_3 of Rabi frequency R_3 we derive the absorptive and dispersive responses of this tunable field. Noticing that both levels $|1\rangle$ and $|3\rangle$ interact with a single pump field only while level $|2\rangle$ is coupled by both pump fields, we consider two situations, (a) the weak field probes $|1\rangle\rightarrow|4\rangle$ transition of frequency ω_{41} [see Fig. 1(a)] and (b) the weak field probes $|2\rangle\rightarrow|4\rangle$ transition of frequency ω_{42} [see Fig. 1(b)].

For the configuration shown in Fig. 1(a), the density matrix equation of motion is given by

$$\dot{\rho}_{11}=\gamma_2\rho_{22}+\gamma_4\rho_{44}+i\chi_1(\rho_{21}-\rho_{12})+i\chi_3(\rho_{41}-\rho_{14}), \tag{1a}$$

$$\dot{\rho}_{22}=-\gamma_2\rho_{22}+\gamma_3\rho_{33}-i\chi_1(\rho_{21}-\rho_{12})+i\chi_2(\rho_{32}-\rho_{23}), \tag{1b}$$

$$\dot{\rho}_{33}=-\gamma_3\rho_{33}-i\chi_2(\rho_{32}-\rho_{23}), \tag{1c}$$

$$\dot{\rho}_{44}=-\gamma_4\rho_{44}-i\chi_3(\rho_{41}-\rho_{14}), \tag{1d}$$

$$\dot{\rho}_{21}=d_{21}\rho_{21}-i\chi_1(\rho_{22}-\rho_{11})+i\chi_2\rho_{31}-i\chi_3\rho_{24}, \tag{1e}$$

$$\dot{\rho}_{31}=d_{31}\rho_{31}-i\chi_1\rho_{32}+i\chi_2\rho_{21}-i\chi_3\rho_{34}, \tag{1f}$$

$$\dot{\rho}_{32}=d_{32}\rho_{32}-i\chi_1\rho_{31}-i\chi_2(\rho_{33}-\rho_{22}), \tag{1g}$$

$$\dot{\rho}_{41}=d_{41}\rho_{41}-i\chi_1\rho_{42}-i\chi_3(\rho_{44}-\rho_{11}), \tag{1h}$$

$$\dot{\rho}_{42}=d_{42}\rho_{42}-i\chi_1\rho_{41}-i\chi_2\rho_{43}+i\chi_3\rho_{12}, \tag{1i}$$

$$\dot{\rho}_{43}=d_{43}\rho_{43}-i\chi_2\rho_{42}+i\chi_3\rho_{13}, \tag{1j}$$

where $\chi_i=R_i/2$, $i=1,2,3$ is half of the Rabi frequencies and the complex detunings d_{ij} are defined as

$$d_{21}=i\delta_{21}-\frac{\gamma_2}{2},\quad d_{31}=i\delta_{31}-\frac{\gamma_3}{2},\quad d_{32}=i\delta_{32}-\frac{\gamma_2+\gamma_3}{2},$$

$$d_{41}=i\delta_{41}-\frac{\gamma_4}{2},\quad d_{42}=i\delta_{42}-\frac{\gamma_2+\gamma_4}{2},$$

$$d_{43}=i\delta_{43}-\frac{\gamma_3+\gamma_4}{2},$$

and the detunings δ_{ij} are defined as

$$\delta_{21}=\omega_1-\omega_{21},\quad \delta_{32}=\omega_2-\omega_{32},\quad \delta_{41}=\omega_3-\omega_{41},$$

$$\delta_{31}=\omega_1+\omega_2-\omega_{31}=\delta_{21}+\delta_{32},$$

$$\delta_{42}=\omega_3-\omega_1-\omega_{42}=\delta_{41}-\delta_{21},$$

$$\delta_{43}=\omega_3-\omega_1-\omega_2-\omega_{43}=\delta_{41}-\delta_{21}-\delta_{32}.$$

To calculate the absorption and dispersion profiles of the field ω_3 probing the ω_{41} transition, it is necessary to obtain a steady-state solution for ρ_{41}. In the limit of weak probe field, it is straightforward to derive a perturbative steady-state solution for ρ_{41} to the first order of χ_3 which can be written as

$$\rho_{41}^{(1)}=\chi_3\,\frac{\chi_1 d_{43}\rho_{12}^{(0)}+i\chi_1\chi_2\rho_{13}^{(0)}-i(d_{42}d_{43}+\chi_2^2)\rho_{11}^{(0)}}{d_{41}d_{42}d_{43}+\chi_1^2 d_{43}+\chi_2^2 d_{41}}, \tag{2}$$

where the steady-state zero-order solutions $\rho_{ij}^{(0)}$ are given in the Appendix.

For the configuration shown in Fig. 1(b), the density matrix equation of motion is given by

$$\dot{\rho}_{11}=\gamma_2\rho_{22}+\gamma_4\rho_{44}+i\chi_1(\rho_{21}-\rho_{12}), \tag{3a}$$

$$\dot{\rho}_{22}=-\gamma_2\rho_{22}+\gamma_3\rho_{33}-i\chi_1(\rho_{21}-\rho_{12})+i\chi_2(\rho_{32}-\rho_{23})+i\chi_3(\rho_{42}-\rho_{24}), \tag{3b}$$

$$\dot{\rho}_{33}=-\gamma_3\rho_{33}-i\chi_2(\rho_{32}-\rho_{23}), \tag{3c}$$

$$\dot{\rho}_{44}=-\gamma_4\rho_{44}-i\chi_3(\rho_{42}-\rho_{24}), \tag{3d}$$

$$\dot{\rho}_{21}=d_{21}\rho_{21}-i\chi_1(\rho_{22}-\rho_{11})+i\chi_2\rho_{31}+i\chi_3\rho_{41}, \tag{3e}$$

$$\dot{\rho}_{31}=d_{31}\rho_{31}-i\chi_1\rho_{32}+i\chi_2\rho_{21}, \tag{3f}$$

$$\dot{\rho}_{32}=d_{32}\rho_{32}-i\chi_1\rho_{31}-i\chi_2(\rho_{33}-\rho_{22})-i\chi_3\rho_{34}, \quad (3g)$$

$$\dot{\rho}_{41}=d_{41}\rho_{41}-i\chi_1\rho_{42}+i\chi_3\rho_{21}, \quad (3h)$$

$$\dot{\rho}_{42}=d_{42}\rho_{42}-i\chi_1\rho_{41}-i\chi_2\rho_{43}-i\chi_3(\rho_{44}-\rho_{22}), \quad (3i)$$

$$\dot{\rho}_{43}=d_{43}\rho_{43}-i\chi_2\rho_{42}+i\chi_3\rho_{23}, \quad (3j)$$

and the complex detunings d_{ij} are defined as

$$d_{21}=i\delta_{21}-\frac{\gamma_2}{2}, \quad d_{31}=i\delta_{31}-\frac{\gamma_3}{2}, \quad d_{32}=i\delta_{32}-\frac{\gamma_2+\gamma_3}{2},$$

$$d_{41}=i\delta_{41}-\frac{\gamma_4}{2}, \quad d_{42}=i\delta_{42}-\frac{\gamma_2+\gamma_4}{2},$$

$$d_{43}=i\delta_{43}-\frac{\gamma_3+\gamma_4}{2},$$

and the detunings δ_{ij} are defined as

$$\delta_{21}=\omega_1-\omega_{21}, \quad \delta_{32}=\omega_2-\omega_{32}, \quad \delta_{42}=\omega_3-\omega_{42},$$

$$\delta_{31}=\omega_1+\omega_2-\omega_{31}=\delta_{21}+\delta_{32},$$

$$\delta_{41}=\omega_3+\omega_1-\omega_{41}=\delta_{42}+\delta_{21},$$

$$\delta_{43}=\omega_3-\omega_2-\omega_{43}=\delta_{42}-\delta_{32}.$$

Likewise, to calculate the absorption and dispersion profiles of the field ω_3 probing the ω_{42} transition, it is necessary to obtain a steady-state solution for ρ_{42}. To the first order of χ_3, the perturbative steady-state solution for ρ_{42} can be written as

$$\rho_{42}^{(1)}=\chi_3\frac{\chi_1 d_{43}\rho_{21}^{(0)}+\chi_2 d_{41}\rho_{23}^{(0)}-i d_{41}d_{43}\rho_{22}^{(0)}}{d_{41}d_{42}d_{43}+\chi_1^2 d_{43}+\chi_2^2 d_{41}}, \quad (4)$$

where the steady-state zero-order solutions $\rho_{ij}^{(0)}$ are given in the Appendix.

Having obtained the analytical solutions as shown in Eqs. (2) and (4) we can calculate both absorption and dispersion profiles for the doubly driven three-level atom. The absorption and dispersion profiles for probing the ω_{41} transition can be obtained by plotting the $\mathrm{Im}[\rho_{41}^{(1)}]$ and $\mathrm{Re}[\rho_{41}^{(1)}]$, respectively, as a function of probe detuning δ_{41}. Likewise, plotting the $\mathrm{Im}[\rho_{42}^{(1)}]$ and $\mathrm{Re}[\rho_{42}^{(1)}]$ as a function of probe detuning δ_{42}, the absorption and dispersion profiles for probing the ω_{42} transition can be obtained. Their numerical results will be presented and discussed in Sec. IV.

III. THE DRESSED-ATOM FORMALISM

The analytical solution obtained in the preceding section allows us to calculate the weak probe field responses for arbitrary values of the parameters and provides a detailed description of how the weak field response is modified by the strong pump fields. Essential as is such a calculation, however, its algebraic complexity prevents us from obtaining a simple physical interpretation. An alternative approach is the so-called dressed-state formalism, which is particularly convenient for describing the photon-atom interaction in the strong field limit. The dressed states are eigenstates of the Hamiltonian of the total system: atom plus photon. Various spectral components correspond to allowed transitions between these dressed states while the heights of various spectral components are determined by the transition strengths and populations associated with the dressed states. Therefore the qualitative trend and general pattern of the complicated spectrum can be predicted, which gives us much better physical insight and allows us to present a clearer interpretation of the numerical results. In this section the dressed-state formalism is introduced to describe the general pattern of the absorption spectrum for the purpose of comparison with the numerical results. Because detailed descriptions of the dressed-state formalism can be found elsewhere [43–45,48,49], we present only a brief description.

A three-level atom interacting with two quasiresonant fields in a cascade scheme is described by a Hamiltonian consisting of an atomic part, a field part, and an interaction part which can be written as

$$H=H_A+H_F+H_I, \quad (5)$$

where

$$H_A=\hbar\omega_{21}|2\rangle\langle 2|+\hbar\omega_{31}|3\rangle\langle 3|, \quad (6a)$$

$$H_F=\hbar\omega_1 a_1^\dagger a_1+\hbar\omega_2 a_2^\dagger a_2, \quad (6b)$$

$$H_1=\frac{\hbar g_1}{2}[a_1|2\rangle\langle 1|+a_1^\dagger|1\rangle\langle 2|]+\frac{\hbar g_2}{2}[a_2|3\rangle\langle 2|+a_2^\dagger|2\rangle\langle 3|], \quad (6c)$$

where a_i and $a_i^\dagger$ are annihilation and creation operators for field modes and g_i is the coupling constant. The ground-state energy is chosen equal to zero. We use notation $|i,n,m\rangle$ to represent the state in which the atom is in level $|i\rangle$ with n photons of field ω_1 and m photons of field ω_2. This state is the eigenstate of the uncoupled atom plus field Hamiltonian, H_A+H_F. Under the quasiresonance condition, levels $|1,n,m\rangle$, $|2,n-1,m\rangle$, and $|3,n-1,m-1\rangle$ become a quasidegenerate triplet and the energy levels of the uncoupled atom plus field form a two-dimensional lattice of such triplets. The interaction Hamiltonian H_1 introduces couplings between levels within the triplet. In the basis of $|1,n,m\rangle$, $|2,n-1,m\rangle$, and $|3,n-1,m-1\rangle$, the matrix representation of the total Hamiltonian H can be written as

$$H-\hat{I}(n\hbar\omega_1+m\hbar\omega_2)=\begin{pmatrix} 0 & \frac{\hbar R_1}{2} & 0 \\ \frac{\hbar R_1}{2} & -\hbar\delta_{21} & \frac{\hbar R_2}{2} \\ 0 & \frac{\hbar R_2}{2} & -\hbar\delta_{21}-\hbar\delta_{32} \end{pmatrix}, \quad (7)$$

where $\hat{I}$ is the identity matrix, the coupling constant g_i is replaced by Rabi frequency R_i, and its photon number de-

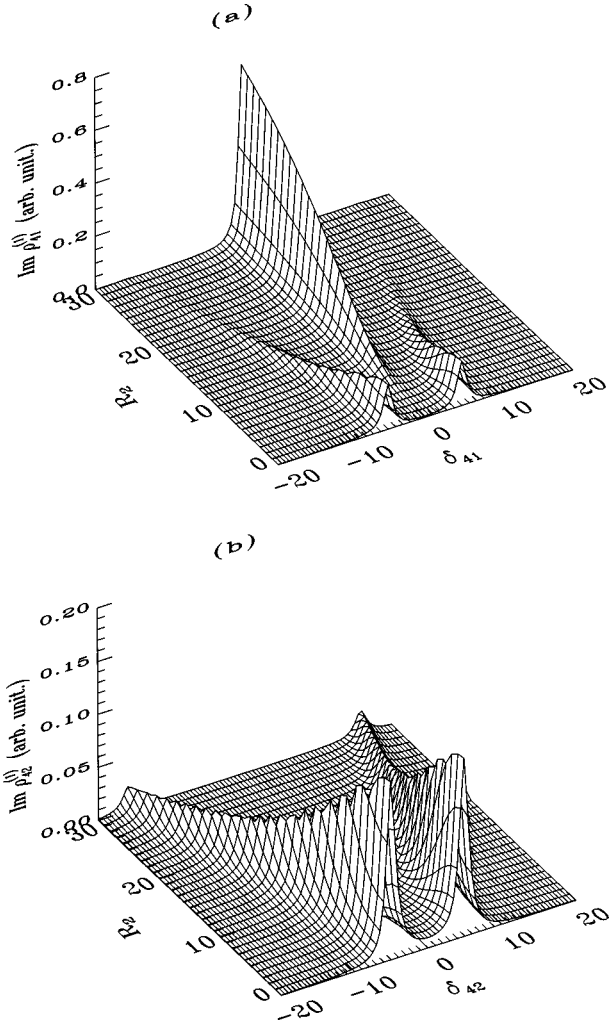

FIG. 2. Calculated absorption spectrum observed on (a) ω_{41} transition and (b) ω_{42} transition for various Rabi frequency of the second driving field R_2 with a resonant pumping: $\delta_{21}=\delta_{32}=0$ and a fixed Rabi frequency of the first driving field: $R_1=10$. The Rabi frequencies R_i and detunings δ_{ij} have been normalized to the relaxation rate γ.

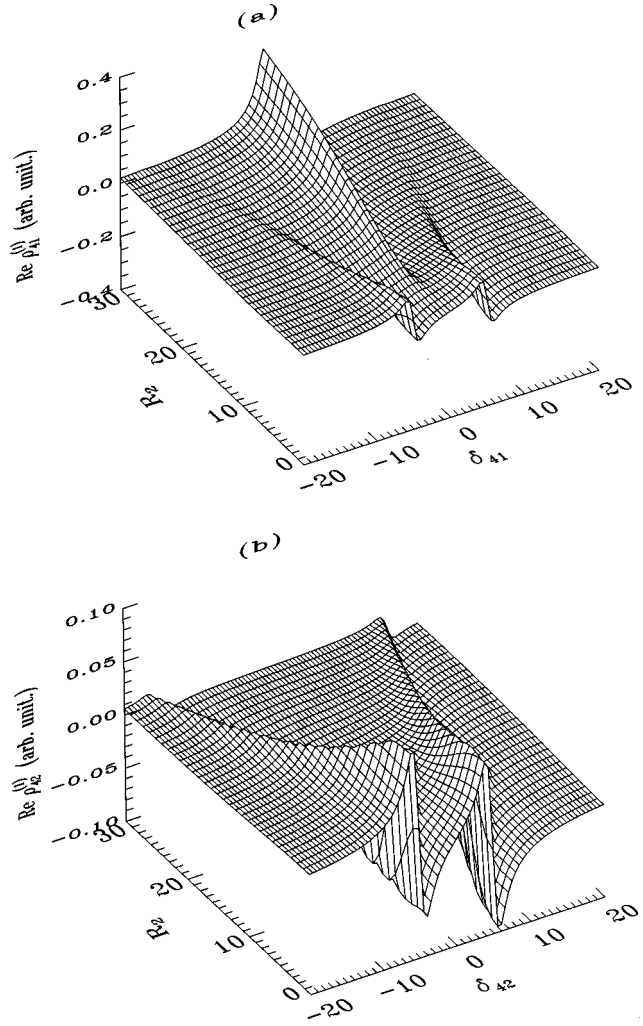

FIG. 3. Calculated dispersion spectrum observed on (a) ω_{41} transition and (b) ω_{42} transition for various Rabi frequency of the second driving field R_2 with a resonant pumping: $\delta_{21}=\delta_{32}=0$ and a fixed Rabi frequency of the first driving field: $R_1=10$. The Rabi frequencies R_i and detunings δ_{ij} have been normalized to the relaxation rate γ.

pendence is neglected in the strong field limit. When taking into account the coupling within the triplet, we obtain three perturbed states: $|a,n,m\rangle$, $|b,n,m\rangle$, and $|c,n,m\rangle$, that are the dressed states. The wave function and the energy of each dressed state can be obtained by diagonalizing the Hamiltonian as given in Eq. (7). In general there are three different eigenvalues and the corresponding dressed states are linear superposition of three unperturbed states: $|1,n,m\rangle$, $|2,n-1,m\rangle$, and $|3,n-1,m-1\rangle$. In particular, for resonant pumping $\delta_{21}=\delta_{32}=0$, a simple calculation yields the dressed-state wave function,

$$|a,n,m\rangle=\frac{1}{\sqrt{2}}\frac{R_1}{R}|1,n,m\rangle+\frac{1}{\sqrt{2}}|2,n-1,m\rangle+\frac{1}{\sqrt{2}}\frac{R_2}{R}|3,n-1,m-1\rangle, \tag{8a}$$

$$|b,n,m\rangle=-\frac{R_2}{R}|1,n,m\rangle+\frac{R_1}{R}|3,n-1,m-1\rangle, \tag{8b}$$

$$|c,n,m\rangle=\frac{1}{\sqrt{2}}\frac{R_1}{R}|1,n,m\rangle-\frac{1}{\sqrt{2}}|2,n-1,m\rangle+\frac{1}{\sqrt{2}}\frac{R_2}{R}|3,n-1,m-1\rangle, \tag{8c}$$

where $R=\sqrt{R_1^2+R_2^2}$, and their corresponding energy is given by

$$E_{a,n,m}=\frac{\hbar R}{2},\quad E_{b,n,m}=0,\quad E_{c,n,m}=-\frac{\hbar R}{2}. \tag{9}$$

The fourth level $|4\rangle$ in dressed-state representation is given by $|d,n,m\rangle=|4,n,m\rangle$, as it is not coupled to the driving fields. It is thus obvious that when probed to the fourth level the general pattern of the absorption spectrum has a three-peak structure, and their positions and relative intensities can be readily derived using the dressed-state picture. This will be discussed in further detail in the next section.

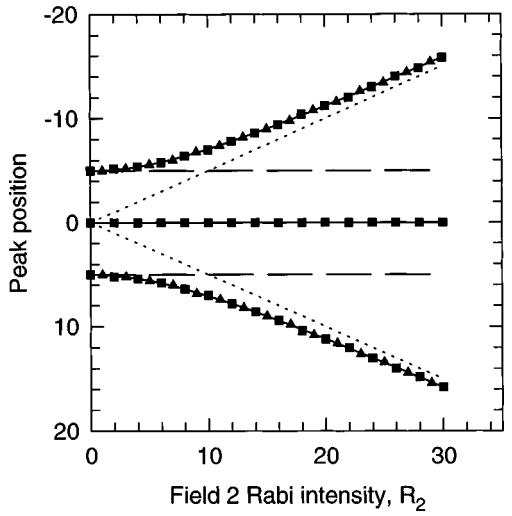

FIG. 4. Peak positions for the spectrum shown in Fig. 2. Data in squares are for ω_{41} transition and data in triangles for ω_{42} transition. Also shown is the result using the dressed-state formalism (curves in solid lines). The dashed straight lines and dotted straight lines indicate the asymptotic behaviors for $R_2 \ll R_1$ and $R_2 \gg R_1$, respectively.

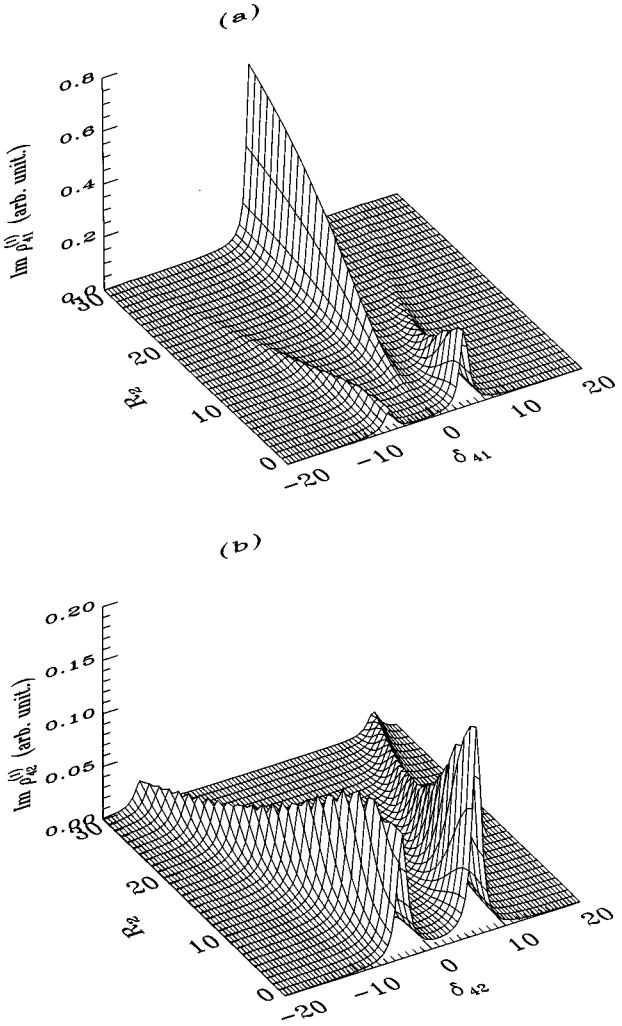

FIG. 5. Calculated absorption spectrum observed on (a) ω_{41} transition and (b) ω_{42} transition for various Rabi frequencies of the second driving field R_2 with a two-photon resonant pumping: $\delta_{21} = -\delta_{32} = -2$ and a fixed Rabi frequency of the first driving field: $R_1 = 10$. The Rabi frequencies R_i and detunings δ_{ij} have been normalized to the relaxation rate γ.

IV. RESULTS AND DISCUSSIONS

In this section we present the results of the numerical calculation and discuss the following situations: (a) the weak field probing the ω_{41} transition where the absorption and dispersion spectrum is given by $\mathrm{Im}[\rho_{41}^{(1)}]$ and $\mathrm{Re}[\rho_{41}^{(1)}]$, respectively, and (b) the weak field probing the ω_{42} transition where the absorption and dispersion spectrum is given by $\mathrm{Im}[\rho_{42}^{(1)}]$ and $\mathrm{Re}[\rho_{42}^{(1)}]$, respectively. As the absorption and dispersion profiles are related to each other through the well-known Kramers-Kronig relationship, we present only one example for the dispersive response while attention is focused on the discussion of the absorptive response. For simplicity, it is assumed that the relaxation rates are the same for all the levels, $\gamma = \gamma_2 = \gamma_3 = \gamma_4$, and pump field Rabi frequencies R_i and detunings δ_{ij} are normalized to the relaxation rate γ.

First, we present the result for the case where both driving fields are resonant: $\delta_{21} = \delta_{32} = 0$. Figure 2(a) shows the absorption profiles probing the ω_{41} transition for various intensities of the second driving field R_2 and a fixed intensity of the first driving field $R_1 = 10$. When $R_2 = 0$ the level $|3\rangle$ is not involved and the configuration of a four-level atom interacting with two pumps and one probe reduces to that of a three-level atom interacting with one pump and one probe. This gives rise to a regular Autler-Townes splitting. However, as the intensity of the second driving field, R_2, increases, the two components of the Autler-Townes doublet initially located at $\delta_{41} = \pm R_1/2$ are split further apart (also see Fig. 4, which plots the peak positions for the spectra shown in Fig. 2 as a function of R_2), in addition, their intensities decrease and finally become negligible in the limit of $R_2 \gg R_1$. More significantly, the second driving field introduces a central component and transforms the well-known Autler-Townes doublet into a triplet. In the limit of $R_2 \gg R_1$ this new spectral component becomes the dominant feature and the spectrum appears to have only a single spectral component as if driving the ω_{32} transition strongly enough decouples the level $|1\rangle$ with the other levels. When probing the ω_{42} transition the corresponding absorption spectra are shown in Fig. 2(b). There are some similarities with the previous spectrum. For example, the Autler-Townes doublet exhibits a similar behavior with an increase of the splitting as R_2 increases. The magnitude of the splitting is identical to that obtained for the previous spectrum. However, there is a remarkable difference between two spectra in that only one of them becomes a triplet [Fig. 2(a)] while the other remains as a doublet [Fig. 2(b)]. It is interesting to note that, although the second driving field does not act directly on level $|1\rangle$, its presence modifies significantly the absorption spectrum observed on the ω_{41} transition: not only increasing the doublet splitting, but introducing an extra peak. On the other hand, the absorption spectrum observed on the ω_{42} transition remains as a doublet exhibiting less modification, even though the level $|2\rangle$ is coupled simultaneously by two pump fields. The correspond-

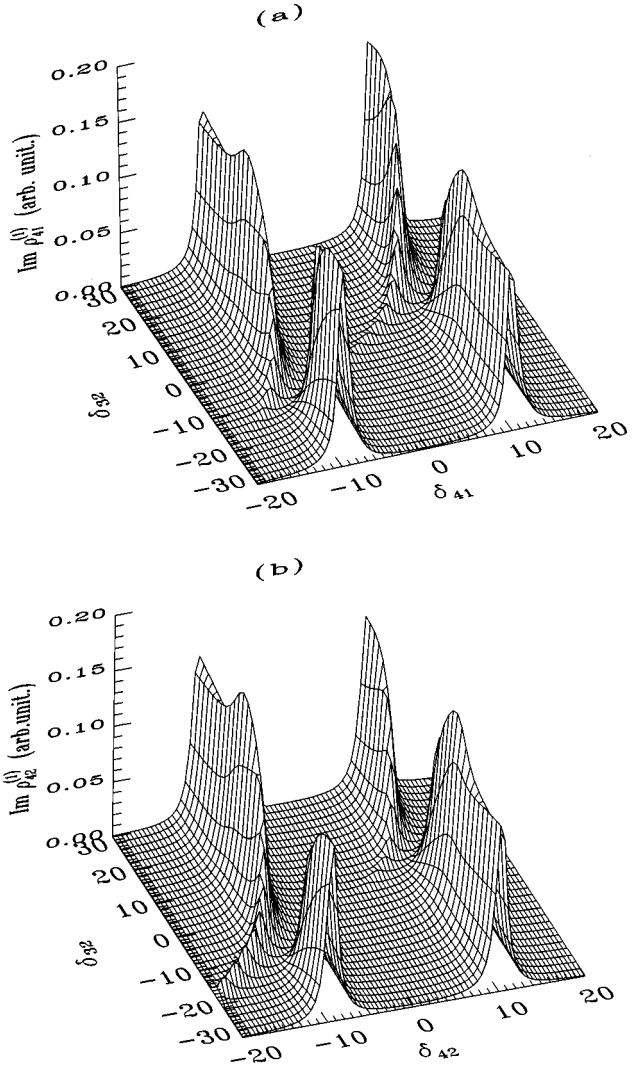

FIG. 6. Calculated absorption spectrum observed on (a) ω_{41} transition and (b) ω_{42} transition for various detunings of the second driving field δ_{32} under the conditions $\delta_{21}=0$, $R_1=20$, and $R_2=8$. The Rabi frequencies R_i and detunings δ_{ij} have been normalized to the relaxation rate γ.

ing dispersive responses are shown in Figs. 3(a) and 3(b) for probing the ω_{41} and ω_{42} transitions, respectively.

The dressed-state formalism gives a clear physical picture as to why the spectrum is modified in such a manner. In general, the doubly driven three-level atom gives rise to a two-dimensional lattice of dressed states and each dressed state is a triplet. This results in an absorption spectrum with a three-peak pattern when probing the doubly driven three-level atom to a fourth level. For the specific situation of resonant pumping as shown in Fig. 2, the positions of these three peaks are at δ_{41} (or δ_{42}) $=0,\pm R/2$ ($R=\sqrt{R_1^2+R_2^2}$) for probing the ω_{41} (or ω_{42}) transition [see Eq. (9)], and this is plotted as a solid line in Fig. 4 which is seen to be in good agreement with the numerical results. It is straightforward to determine the transition strengths and populations associated with the dressed states and obtain the intensity of various spectral components. Taking the resonant pumping case as an example, when the ω_{41} transition is probed the allowed transition is that between level $|4,n,m\rangle$ and $|1,n,m\rangle$, and in the dressed-state picture the transition occurs between level $|d,n,m\rangle$ and triplet: $|a,n,m\rangle$, $|b,n,m\rangle$ and $|c,n,m\rangle$. As each of the triplet states contain $|1,n,m\rangle$ [see Eq. (8)], there are three allowed transitions, which results in a three-peaked spectrum. On the other hand, when the ω_{42} transition is probed the allowed transition is that between $|4,n,m\rangle$ and $|2,n,m\rangle$ levels, and in the dressed-state picture the transition occurs between level $|d,n,m\rangle$ and triplet: $|a,n+1,m\rangle$, $|b,n+1,m\rangle$, and $|c,n+1,m\rangle$. The central component of the triplet $|b,n+1,m\rangle$ does not contain $|2,n,m\rangle$, hence, a doublet is observed rather than a triplet. In fact, using the dressed-state formalism it is simple to prove that this is true even for nonresonant pumping provided that the pump detunings satisfy a general two-photon resonance condition, $\delta_{31}=\delta_{21}+\delta_{32}=0$ or $\delta_{21}=-\delta_{32}$. This is illustrated in Fig. 5 for conditions $R_1=10$, $\delta_{21}=-2$, and $\delta_{32}=2$, where traces (a) correspond to probing the ω_{41} transition and traces (b) to the ω_{42} transition. The former gives a three-peaked spectrum whereas the latter gives a two-peaked spectrum.

We have shown that under the resonant pumping $\delta_{21}=\delta_{32}=0$ or more generally under the two-photon resonant pumping $\delta_{31}=\delta_{21}+\delta_{32}=0$ the second driving field ω_2 introduces an extra component at zero detuning of the probe field ω_3 when probing the ω_{41} transition but not when probing the ω_{42} transition. In what follows we discuss the changes of the absorption spectrum as a function of the second driving field detuning δ_{32} while keeping the first driving field resonant: $\delta_{21}=0$. The spectrum is calculated for the situation $R_1>R_2$ ($R_1=20$ and $R_2=8$) and the result is shown in Fig. 6(a) for probing the ω_{41} transition and Fig. 6(b) for probing the ω_{42} transition. When the second driving field has a zero detuning, $\delta_{32}=0$, the absorption spectrum exhibits a triplet and doublet splitting for probing the ω_{41} and ω_{42} transition, respectively. As the second driving field frequency is detuned from the resonance, the central component associated with the second driving field is continuously displaced from zero probe detuning and in both cases gains intensity. Thus in both cases the spectrum has a triplet structure. When the second driving field detuning δ_{32} approaches $\pm R_1/2$, there is an anticrossing between the states associated with one of the Autler-Townes components and the displaced central component. This leads to a further splitting which will be discussed later. For very large detuning, δ_{32}, the second driving field introduces neg-

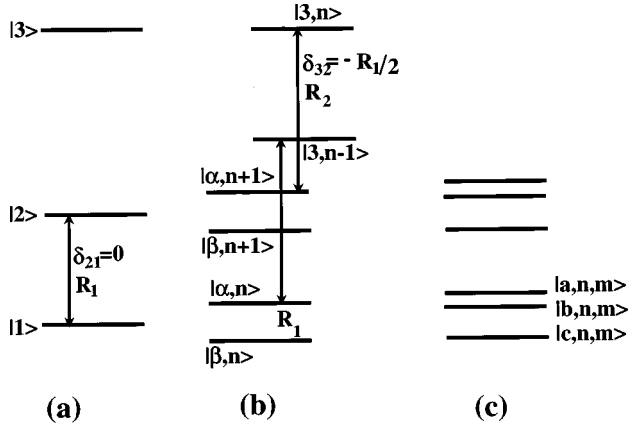

FIG. 7. Energy level scheme illustrating the doubly dressed state.

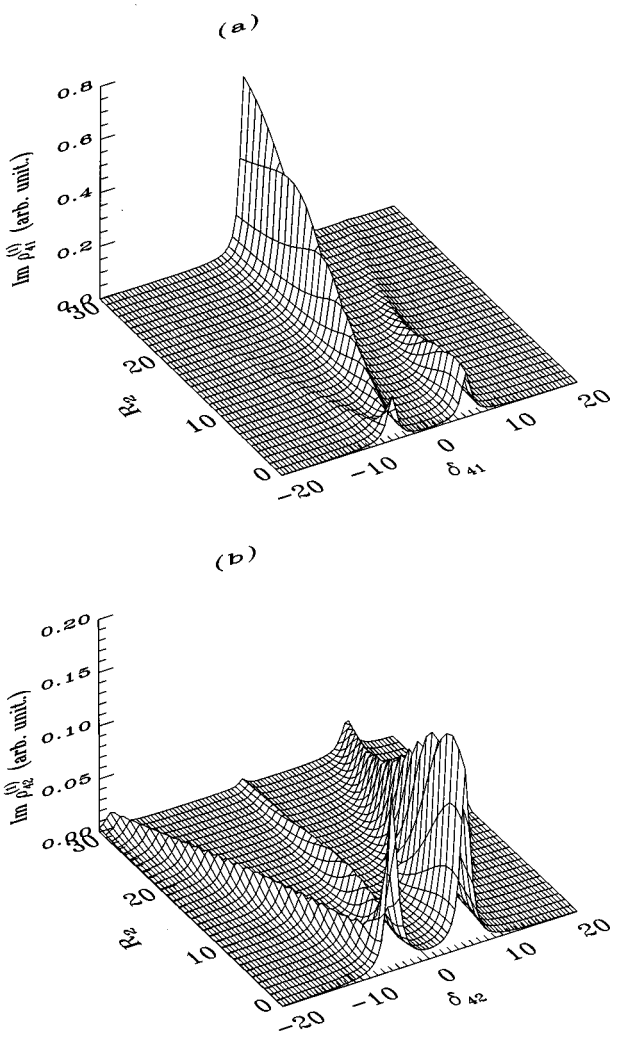

FIG. 8. Calculated absorption spectrum observed on (a) ω_{41} transition and (b) ω_{42} transition for various Rabi frequency of the second driving field R_2 under the conditions $\delta_{21}=0$, $R_1=10$, and $\delta_{32}=-R_1/2=-5$. The Rabi frequencies R_i and detunings δ_{ij} have been normalized to the relaxation rate γ.

ligible modification to the probe field response and the predominant feature of the absorption spectrum is an Autler-Townes doublet associated with driving the ω_{21} transition with a resonant field ω_1.

The doublet formed when $\delta_{32}\approx\pm R_1/2$ as shown above is best discussed in terms of the doubly dressed states as illustrated in Fig. 7 for the $\delta_{32}=-R_1/2$ case. In the limit of $R_2 \ll R_1$, instead of diagonalizing the total atom plus photon Hamiltonian, the dressed states can be obtained by the following steps. First we consider the resonant strong field ω_1 [see Fig. 7(a)] and the singly dressed states are given in Fig. 7(b). From this figure it can be seen that when the second driving field ω_2 is introduced with a detuning $\delta_{32}=-R_1/2$ it will be resonant with the single dressed-state transition: $|3,n-1>\leftrightarrow|\alpha,n>$, where $|\alpha,n>=(1/\sqrt{2})(|1,n>+|2,n-1>)$. This interaction gives rise to a doubly dressed state with a splitting of $R_2/\sqrt{2}$ [see Fig. 7(c)]. In this doubly dressed-state description there is an anticrossing of the states as the detuning is varied and this leads to the trends shown in Figs. 6(a) and 6(b) and in particular the doublet at $\delta_{32}\approx\pm R_1/2$.

The absorption spectrum at the anticrossing region is investigated further as a function of the intensity of the second driving field R_2 for the specific case of $R_1=10$, $\delta_{21}=0$, and $\delta_{32}=-R_1/2=-5$. The result is shown in Fig. 8 for probing (a) the ω_{41} and (b) the ω_{42} transition. In the absence of the second driving field the spectrum is simply an Autler-Townes doublet associated with the first driving field with two peaks at $\pm R_1/2$. Introducing the second driving field causes a doublet splitting in one of these two peaks and results in a three-peaked spectrum. The peak positions of these three spectral components are plotted in Fig. 9 as a function of R_2, and are again in good agreement with the prediction of the dressed-state formalism (solid lines in Fig. 9). In particular, when the second driving field is weak ($R_2<R_1$), there is a linear splitting proportional to $R_2/\sqrt{2}$ in one of the Autler-Townes components (see dashed lines in Fig. 9). On the other hand, with a very large R_2 ($R_2\gg R_1$) the position of the inner component approaches zero detuning, and the two outer components approach a linear splitting proportional to R_2. The energies of the dressed states associated with the ground and intermediate states are directly related and, hence there is a one-to-one correlation in the peak positions in the respective spectrum as shown in Figs. 8(a) and 8(b). However, the intensity patterns are very different for probing different transitions. When the second driving field is weak ($R_2<R_1$), the spectrum is comprised of a regular Autler-Townes splitting caused by the first driving field and one of the two components split further by the second driving field. As the second driving field intensity increases, in the case of probing the ω_{41} transition the inner component gains intensity and becomes dominant [Fig. 8(a)], and for very large R_2 ($R_2\gg R_1$) the second driving field totally decouples the ground state as was the case in the resonant pumping situation. On the other hand, when probing the ω_{42} transition, as the second driving field intensity increases, the inner component loses intensity and becomes negligible

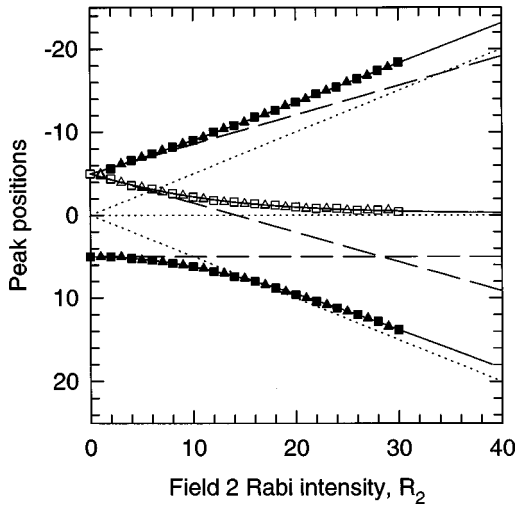

FIG. 9. Peak positions for the spectrum shown in Fig. 8. Data in squares are for probing the ω_{41} transition and data in triangles for ω_{42} transition. Also shown is the result using the dressed-state formalism (curves in solid lines). The dashed straight lines and dotted straight lines indicate the asymptotic behaviors for $R_2\ll R_1$ and $R_2\gg R_1$.

[Fig. 8(b)], and for very large R_2, the spectrum approaches that for a regular Autler-Townes spectrum with a splitting of R_2.

V. CONCLUSIONS

In this paper we study the ac Stark effect of a doubly driven three-level atom. We derive analytical expressions for the absorption and dispersion profiles of a weak field probing the doubly driven three-level atom to a fourth level and calculate the absorption spectrum for various parameters. We show that the general feature of the absorption spectrum has a triplet structure and the position and intensity of each component of the triplet depend on the intensities and detunings of the driving fields. In particular, when the driving fields satisfy a two-photon resonance condition, we observe an interesting phenomenon where the central component of the triplet has a zero intensity when probing the intermediate level. Finally we show that a simple physical picture of the overall pattern of the numerical results can be obtained using the dressed-state formalism.

ACKNOWLEDGMENTS

C. W. wishes to thank the Australian Research Council and the University of Dortmund for financial support.

APPENDIX

The density matrix equations of motion to zero order of weak probe field χ_3 are the same for both configurations shown in Figs. 1(a) and 1(b), which can be written as

$$\dot{\rho}_{11}^{(0)} = \gamma_2\rho_{22}^{(0)} + \gamma_4\rho_{44}^{(0)} + i\chi_1(\rho_{21}^{(0)} - \rho_{12}^{(0)}), \tag{A1a}$$

$$\dot{\rho}_{22}^{(0)} = -\gamma_2\rho_{22}^{(0)} + \gamma_3\rho_{33}^{(0)} - i\chi_1(\rho_{21}^{(0)} - \rho_{12}^{(0)}) + i\chi_2(\rho_{32}^{(0)} - \rho_{23}^{(0)}), \tag{A1b}$$

$$\dot{\rho}_{33}^{(0)} = -\gamma_3\rho_{33}^{(0)} - i\chi_2(\rho_{32}^{(0)} - \rho_{23}^{(0)}), \tag{A1c}$$

$$\dot{\rho}_{44}^{(0)} = -\gamma_4\rho_{44}^{(0)}, \tag{A1d}$$

$$\dot{\rho}_{21}^{(0)} = d_{21}\rho_{21}^{(0)} - i\chi_1(\rho_{22}^{(0)} - \rho_{11}^{(0)}) + i\chi_2\rho_{31}^{(0)}, \tag{A1e}$$

$$\dot{\rho}_{31}^{(0)} = d_{31}\rho_{31}^{(0)} - i\chi_1\rho_{32}^{(0)} + i\chi_2\rho_{21}^{(0)}, \tag{A1f}$$

$$\dot{\rho}_{32}^{(0)} = d_{32}\rho_{32}^{(0)} - i\chi_1\rho_{31}^{(0)} - i\chi_2(\rho_{33}^{(0)} - \rho_{22}^{(0)}), \tag{A1g}$$

$$\dot{\rho}_{41}^{(0)} = d_{41}\rho_{41}^{(0)} - i\chi_1\rho_{42}^{(0)}, \tag{A1h}$$

$$\dot{\rho}_{42}^{(0)} = d_{42}\rho_{42}^{(0)} - i\chi_1\rho_{41}^{(0)} - i\chi_2\rho_{43}^{(0)}, \tag{A1i}$$

$$\dot{\rho}_{43}^{(0)} = d_{43}\rho_{43}^{(0)} - i\chi_2\rho_{42}^{(0)}. \tag{A1j}$$

In the steady-state limit, the above equations can be solved exactly as

$$\rho_{11}^{(0)} = 1 - \rho_{22}^{(0)} - \rho_{33}^{(0)} - \rho_{44}^{(0)}, \tag{A2a}$$

$$\rho_{22}^{(0)} = \chi_1^2 \frac{2\,\mathrm{Re}(Z_{21})[2\chi_2^2\,\mathrm{Re}(Y_{32}) - \gamma_3] - 4\chi_2^2\mathrm{Re}(Y_{21})\mathrm{Re}(Z_{32})}{[\gamma_2 - 2\chi_1^2\,\mathrm{Re}(X_{21})][2\chi_2^2\,\mathrm{Re}(Y_{32}) - \gamma_3] + 4\chi_1^2\chi_2^2\,\mathrm{Re}(X_{32})\mathrm{Re}(Y_{21})}, \tag{A2b}$$

$$\rho_{33}^{(0)} = \chi_2^2 \frac{2\,\mathrm{Re}(Z_{32})[2\chi_1^2\,\mathrm{Re}(X_{21}) - \gamma_2] - 4\chi_1^2\,\mathrm{Re}(X_{32})\mathrm{Re}(Z_{21})}{[\gamma_2 - 2\chi_1^2\,\mathrm{Re}(X_{21})][2\chi_2^2\,\mathrm{Re}(Y_{32}) - \gamma_3] + 4\chi_1^2\chi_2^2\,\mathrm{Re}(X_{32})\mathrm{Re}(Y_{21})}, \tag{A2c}$$

$$\rho_{21}^{(0)} = i\chi_1(X_{21}\rho_{22}^{(0)} + Y_{21}\rho_{33}^{(0)} + Z_{21}), \tag{A2d}$$

$$\rho_{31}^{(0)} = \chi_1\chi_2(X_{31}\rho_{22}^{(0)} + Y_{31}\rho_{33}^{(0)} + Z_{31}), \tag{A2e}$$

$$\rho_{32}^{(0)} = i\chi_2(X_{32}\rho_{22}^{(0)} + Y_{32}\rho_{33}^{(0)} + Z_{32}), \tag{A2f}$$

$$\rho_{44}^{(0)} = \rho_{41}^{(0)} = \rho_{42}^{(0)} = \rho_{43}^{(0)} = 0, \tag{A2g}$$

where

$$X_{21}=\frac{2d_{31}d_{32}+2\chi_1^2-\chi_2^2}{D},\quad X_{31}=\frac{2d_{32}+d_{21}}{D},$$

$$X_{32}=\frac{-d_{21}d_{31}+2\chi_1^2-\chi_2^2}{D},\quad Y_{21}=\frac{d_{31}d_{32}+\chi_1^2+\chi_2^2}{D},$$

$$Y_{31}=\frac{d_{32}-d_{21}}{D},\quad Y_{32}=\frac{d_{21}d_{31}+\chi_1^2+\chi_2^2}{D},$$

$$Z_{21}=-\frac{d_{31}d_{32}+\chi_1^2}{D},\quad Z_{31}=-\frac{d_{32}}{D},\quad Z_{32}=-\frac{\chi_1^2}{D},$$

and $D=d_{21}d_{31}d_{32}+\chi_1^2d_{21}+\chi_2^2d_{32}$.

[1] L. Allen and J. H. Eberly, *Optical Resonance and Two Level Atoms* (Dover, New York, 1987).
[2] P. Meystre and M. Sargent III, *Elements of Quantum Optics* (Springer-Verlag, Berlin, 1991).
[3] M. D. Levenson and S. S. Kano, *Introduction to Nonlinear Laser Spectroscopy* (Academic, New York, 1988).
[4] B. R. Mollow, Phys. Rev. **188**, 1969 (1969).
[5] F. Y. Wu, R. E. Grove, and S. Ezekiel, Phys. Rev. Lett. **35**, 1426 (1975).
[6] R. E. Grove, F. Y. Wu, and S. Ezekiel, Phys. Rev. A **15**, 227 (1977).
[7] B. R. Mollow, Phys. Rev. A **5**, 2217 (1972).
[8] F. Y. Wu, S. Ezekiel, M. Docloy, and B. R. Mollow, Phys. Rev. Lett. **38**, 1077 (1977).
[9] R. W. Boyd, M. G. Raymer, P. Narum, and D. J. Harter, Phys. Rev. A **24**, 411 (1981).
[10] A. M. Bonch-Bruevich, V. A. Khodovoi, and N. A. Chigir, Zh. Eksp. Teor. Fiz. **67**, 2069 (1974) [Sov. Phys. JETP **40**, 1027 (1975)].
[11] Y. Zhu, Q. Wu, S. Morin, and T. W. Mossberg, Phys. Rev. Lett. **65**, 1200 (1990).
[12] S. Papademetriou, S. Chakmakjian, and C. R. Stroud, Jr., J. Opt. Soc. Am. B **9**, 1182 (1992).
[13] C. Wei and N. B. Manson, Phys. Rev. A **49**, 4751 (1994).
[14] N. B. Manson, C. Wei, and J. P. D. Martin, Phys. Rev. Lett. **76**, 3943 (1996).
[15] See Chapter 8 of Ref. [2].
[16] S. H. Autler and C. H. Townes, Phys. Rev. **100**, 703 (1955).
[17] F. Shuda, C. R. Stroud, Jr., and M. Hercher, J. Phys. B **7**, L198 (1974).
[18] J. L. Picque and J. Pinard, J. Phys. B **9**, L77 (1976).
[19] H. R. Gray and C. R. Stroud, Jr., Opt. Commun. **25**, 359 (1978).
[20] P. R. Hemmer, B. W. Peuse, F. Y. Wu, J. E. Thomas, and S. Ezekiel, Opt. Lett. **6**, 531 (1981).
[21] C. Wei, N. B. Manson, and J. P. D. Martin, Phys. Rev. A **51**, 1438 (1995).
[22] G. Alzetta, A. Gozzini, L. Moi, and G. Orriols, Nuovo Cimento B **36**, 5 (1976).
[23] R. M. Whitley and C. R. Stroud, Jr., Phys. Rev. A **14**, 1498 (1976).
[24] E. Arimondo and G. Orriols, Lett. Nuovo Cimento **17**, 333 (1976).
[25] H. R. Gray, R. M. Whitley, and C. R. Stroud, Jr., Opt. Lett. **3**, 218 (1978).
[26] G. Orriols, Nuovo Cimento B **53**, 1 (1979).
[27] P. M. Radmore and P. L. Knight, J. Phys. B **15**, 561 (1982).
[28] A. Imamoglu and S. E. Harris, Opt. Lett. **14**, 1344 (1989).
[29] S. E. Harris, Phys. Rev. Lett. **62**, 1033 (1989).
[30] K.-J. Boller, A. Imamoglu, and S. E. Harris, Phys. Rev. Lett. **66**, 2593 (1991).
[31] J. E. Field, K. H. Hahn, and S. E. Harris, Phys. Rev. Lett. **67**, 3062 (1991).
[32] M. Xiao, Y. Li, S. Jin, and J. Gea-Banacloche, Phys. Rev. Lett. **74**, 666 (1995).
[33] Y. Li and M. Xiao, Phys. Rev. A **51**, R2703 (1995).
[34] O. Kocharovskaya, Phys. Rep. **219**, 175 (1992).
[35] A. S. Zibrov, M. D. Lukin, D. E. Nikonov, L. Hollberg, M. O. Scully, V. L. Velichansky, and H. G. Robinson, Phys. Rev. Lett. **75**, 1499 (1995).
[36] See also a recent review article and references cited therein, E. Arimondo, in *Progress in Optics*, edited by E. Wolf (Elsevier, Amsterdam, 1996), Vol. XXXV.
[37] M. F. Van leeuwen, S. Papademetriou, and C. R. Stroud, Jr., Phys. Rev. A **53**, 990 (1996).
[38] S. Papademetriou, M. F. Van leeuwen, and C. R. Stroud, Jr., Phys. Rev. A **53**, 997 (1996).
[39] Z. Ficek and H. S. Freedhoff, Phys. Rev. A **48**, 3092 (1993).
[40] N. B. Manson, C. Wei, S. A. Holmstrom, and J. P. D. Martin, Laser Phys. **5**, 486 (1995).
[41] L. M. Narducci, M. O. Scully, G. L. Oppo, P. Ru, and J. R. Tredicce, Phys. Rev. A **42**, 1630 (1990).
[42] A. S. Manka, H. M. Doss, L. M. Narducci, P. Ru, and G. L. Oppo, Phys. Rev. A **43**, 3748 (1991).
[43] C. Cohen-Tannoudji and S. Reynaud, J. Phys. B **10**, 345 (1977).
[44] C. Cohen-Tannoudji and S. Reynaud, J. Phys. B **10**, 365 (1977).
[45] C. Cohen-Tannoudji and S. Reynaud, J. Phys. B **10**, 2311 (1977).
[46] S. N. Sandhya and K. K. Sharma, Phys. Rev. A **55**, 2155 (1997).
[47] S. M. Sadeghi, J. Meyer, and H. Rastegar, Phys. Rev. A **56**, 3097 (1997).
[48] P. R. Berman and R. Salomaa, Phys. Rev. A **25**, 2667 (1982).
[49] C. Cohen-Tannoudji, J. Dupont-Roc, and G. Grynberg, *Atom-Photon Interactions: Basic Processes and Applications* (Wiley, New York, 1992).